Available online at www.sciencedirect.com
SCIENCE DIRECT®
Journal of Sound and Vibration 292 (2006) 1015–1030
JOURNAL OF SOUND AND VIBRATION
www.elsevier.com/locate/jsvi

Short Communication

Numerical investigation of the modal sensitivity of suspended cables with localized damage

Najib Bouaanani*

Department of Civil, Geological and Mining Engineering, École Polytechnique de Montréal, Montreal, Que., Canada H3C 3A7

Received 2 August 2004; received in revised form 17 June 2005; accepted 13 September 2005
Available online 17 November 2005

Abstract

This paper examines the effect of damage location and size on the modal sensitivity of suspended cables. A numerical finite difference approach that takes account of sag-extensibility and bending stiffness is programmed and adapted to investigate the modal behaviour of suspended cables with induced damage. The finite difference program developed is used to conduct an extensive parametric study on 12 cables with different combinations of sag-extensibility and bending stiffness parameters. A systematic study of the dynamic behaviour of the cables under various damage cases is carried out and original findings are thoroughly discussed. It is shown that despite the complexity of the relationship between damage and the dynamic properties of the cables, definite trends could be identified, especially for out-of-plane vibrations.

1. Introduction

Cables are widely used as structural elements especially when lightness, flexibility and aesthetics are key design factors. However, cable structures including overhead transmission lines, cable-supported roofs, guyed towers, suspension and cable-stayed bridges are generally exposed to wind, rain, ice and long-term fatigue during their design life. Subjected to such loadings, the cables become increasingly vulnerable to damage and deterioration, making their condition assessment a priority to prevent premature or catastrophic failure.

Considerable research has been devoted to the general design and analysis of cable structures and a thorough account of these investigations can be found in Refs. [1–3]. Cable forces have been frequently estimated from measured natural frequencies and practical formulas have been developed for this purpose [4]. However, only recently have the combined effects of sag-extensibility and bending stiffness been fully and efficiently considered in the analysis [5,6]. Most of the literature focuses on the dynamic analysis of cables of uniform sections. To the author's knowledge, there is no published work dedicated to a systematic study of the dynamic behaviour of a suspended cable under the effect of a localized damage. The aim of the present paper is to investigate the relationship between damage location, damage size, and the corresponding changes in the natural frequencies and mode shapes of suspended cables. To this end, a finite difference scheme originally proposed by Mehrabi and Tabatabai [5] is programmed and adapted herein to analyse the in-plane

*Tel.: +1 514 340 4711x3971; fax: +1 514 340 5881.
E-mail address: najib.bouaanani@polymtl.ca.

0022-460X/$ - see front matter © 2005 Elsevier Ltd. All rights reserved.
doi:10.1016/j.jsv.2005.09.013

and out-of-plane free vibrations of cables with varied properties to cover a wide range. Salient features of the modal response are thoroughly discussed.

2. Finite difference formulation

The finite difference formulation used is based on an accurate mathematical model, taking account of sag-extensibility and bending stiffness effects. Only the basic elements of the formulation are briefly reviewed for convenient reference in this section. A detailed description of the method can be found in Ref. [5].

2.1. Static profile

The horizontal span suspended cable shown in Fig. 1 is in equilibrium under the effect of its own weight uniformly distributed along its arc length. Considering a differential horizontal length dx of the cable, and neglecting the effects of axial rigidity and sag on the static profile, equilibrium of forces yields the following differential equation governing the static deflected shape z

$$\frac{\mathrm{d}^2}{\mathrm{d}x^2}\left(EI\frac{\mathrm{d}^2 z}{\mathrm{d}x^2}\right) - H_s\frac{\mathrm{d}^2 z}{\mathrm{d}x^2} - mg = 0 \tag{1}$$

in which EI is the cable bending rigidity; H_s the horizontal component of the static cable tension; g the gravitational acceleration; mg the cable weight per unit length and x a horizontal Cartesian coordinates system with origin located at the left support of the cable. Eq. (1) is subject to the boundary conditions

$$z(0) = 0, \quad z(L) = 0. \tag{2}$$

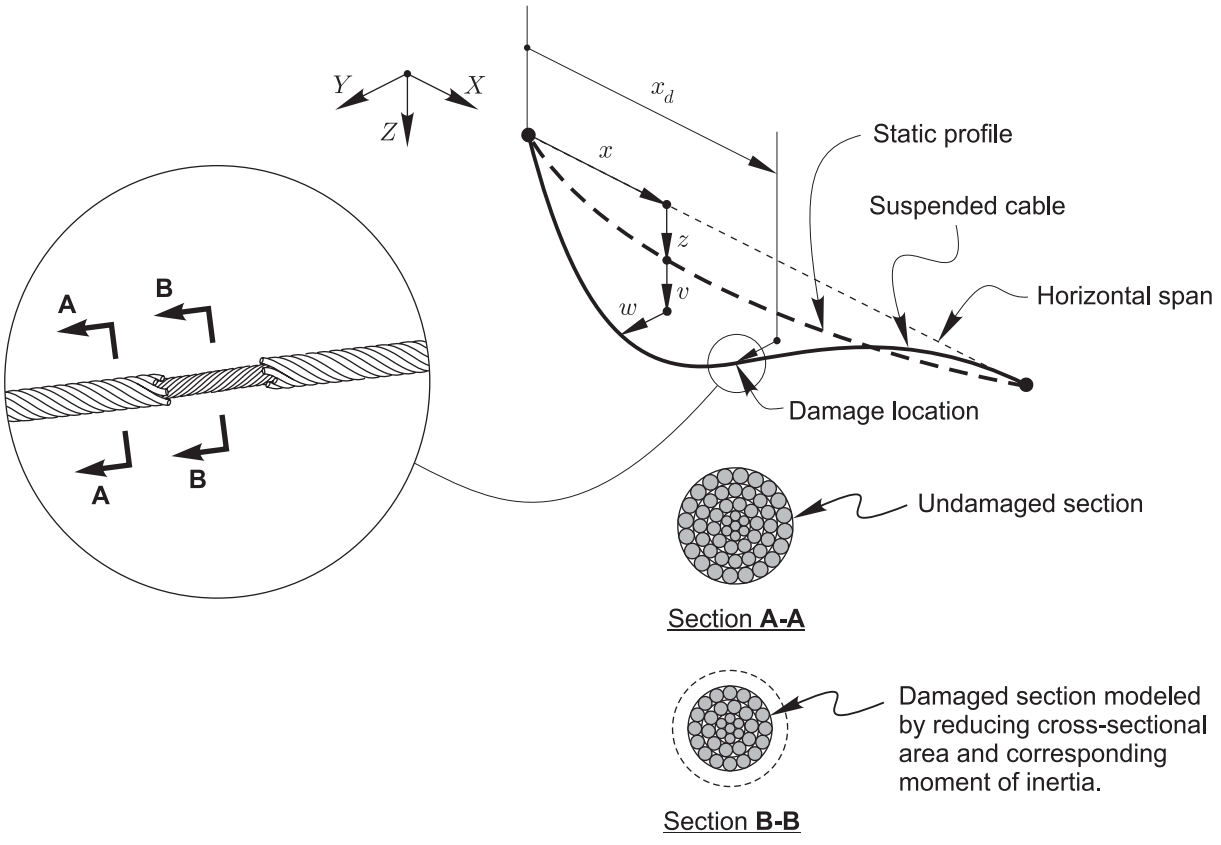

Fig. 1. Static and dynamic analysis of a damaged suspended cable.

Using a central finite difference scheme, Eq. (1) is transformed into a system of linear equations that can be cast in a matrix form

$$\mathbf{K}_s\mathbf{z} = g\mathbf{m}, \tag{3}$$

where $\mathbf{z}$ is a vector containing the static deflections z_i, $i = 1, \ldots, n$, n being the number of nodes in the discretized cable. The mass vector $\mathbf{m}$ and static stiffness matrix $\mathbf{K}_s$ are defined by

$$\mathbf{m}^{\mathrm{T}} = [m_1, m_2, \ldots, m_i, \ldots, m_n], \tag{4}$$

$$\mathbf{K}_s = \begin{bmatrix} [\alpha_1 + (-1)^p\beta_1] & \kappa_1 & \gamma_1 & 0 & \ldots & \ldots & \ldots & \ldots & \ldots & \ldots & 0 \\ \eta_2 & \alpha_2 & \kappa_2 & \gamma_2 & 0 & \ldots & \ldots & \ldots & \ldots & \ldots & 0 \\ -\beta_3 & \eta_3 & \alpha_3 & \kappa_3 & \gamma_3 & 0 & \ldots & \ldots & \ldots & \ldots & 0 \\ 0 & \ldots & 0 & -\beta_i & \eta_i & \alpha_i & \kappa_i & \gamma_i & 0 & \ldots & 0 \\ 0 & \ldots & \ldots & \ldots & \ldots & \ldots & 0 & -\beta_{n-1} & \eta_{n-1} & \alpha_{n-1} & \kappa_{n-1} \\ 0 & \ldots & \ldots & \ldots & \ldots & \ldots & \ldots & 0 & -\beta_n & \eta_n & [\alpha_n + (-1)^{p+1}\gamma_n] \end{bmatrix}, \tag{5}$$

where m_i is the mass per unit length, $p = 1$ for fixed end condition, $p = 2$ for pinned end condition and where for $i = 1, \ldots, n$

$$\begin{aligned} \alpha_i &= -\frac{2}{a^4}(EI_{i+1} - 5EI_i + EI_{i-1}) + \frac{2H_s}{a^2}, \\ \beta_i &= \frac{1}{2a^4}(EI_{i+1} - 2EI_i - EI_{i-1}), \\ \gamma_i &= \frac{1}{2a^4}(EI_{i+1} + 2EI_i - EI_{i-1}), \\ \kappa_i &= -\frac{2}{a^4}(3EI_i - EI_{i-1}) - \frac{H_s}{a^2}, \\ \eta_i &= \frac{2}{a^4}(EI_{i+1} - 3EI_i) - \frac{H_s}{a^2}. \end{aligned} \tag{6}$$

Eq. (3) is solved numerically herein using Gaussian elimination.

2.2. Dynamic behaviour

The horizontal span suspended cable is now subjected to small in-plane and out-of-plane vibrations around its static profile. Again, the equations of motion result from equilibrium of forces of a differential horizontal length dx of the cable

$$\frac{\partial^2}{\partial x^2}\left(EI\frac{\partial^2 v}{\partial x^2}\right) - H_s\frac{\partial^2 v}{\partial x^2} - H_d\frac{\mathrm{d}^2 z}{\mathrm{d}x^2} + m\frac{\partial^2 v}{\partial t^2} = 0, \tag{7}$$

$$\frac{\partial^2}{\partial x^2}\left(EI\frac{\partial^2 w}{\partial x^2}\right) - H_s\frac{\partial^2 w}{\partial x^2} + m\frac{\partial^2 w}{\partial t^2} = 0, \tag{8}$$

in which v and w are the in-plane and out-of-plane components of cable motion, respectively, and H_d the dynamic horizontal cable tension. It is worth to mention that the in-plane and out-of-plane motions are assumed to be uncoupled due to the absence of horizontal static load and that the longitudinal component of cable motion is also neglected.

Expressing the displacements in terms of their complex-valued frequency responses and using the separation of variables technique derived by Mehrabi and Tabatabai [5], Eqs. (7) and (8) are transformed into two

eigenvalue problems

$$\frac{d^2(EI)}{dx^2}\frac{d^2\bar{v}}{dx^2}+2\frac{d(EI)}{dx}\frac{d^3\bar{v}}{dx^3}+EI\frac{d^4\bar{v}}{dx^4}-H_s\frac{d^2\bar{v}}{dx^2}+\frac{\int_0^L(d^2z/dx^2)\bar{v}\,dx}{\int_0^L\frac{[(dz/dx)^2+1]^{3/2}}{EA}dx}-m\omega^2\bar{v}=0, \tag{9}$$

$$\frac{d^2(EI)}{dx^2}\frac{d^2\bar{w}}{dx^2}+2\frac{d(EI)}{dx}\frac{d^3\bar{w}}{dx^3}+EI\frac{d^4\bar{w}}{dx^4}-H_s\frac{d^2\bar{w}}{dx^2}-m\omega^2\bar{w}=0, \tag{10}$$

where $\bar{v}$ and $\bar{w}$ are the frequency response functions of v and w, respectively.

Again using central difference discretization, the two differential equations are transformed to yield two systems of equations

$$\mathbf{K}_v\bar{\mathbf{v}}=\omega_v^2\mathbf{M}\bar{\mathbf{v}}, \tag{11}$$

$$\mathbf{K}_w\bar{\mathbf{w}}=\omega_w^2\mathbf{M}\bar{\mathbf{w}}, \tag{12}$$

where ω_v and ω_w are the in-plane and out-of-plane eigenfrequencies, $\mathbf{M}$ is a square matrix with nodal mass vector $\mathbf{m}$ elements on the diagonal and zero elsewhere, and $\mathbf{K}_v$ and $\mathbf{K}_w$ are defined by

$$\mathbf{K}_v=\mathbf{K}_s+\mathbf{r}\mathbf{s}^{\mathrm{T}}, \tag{13}$$

$$\mathbf{K}_w=\mathbf{K}_s \tag{14}$$

in which $\mathbf{K}_s$ is the static stiffness matrix defined in Eq. (5), and vectors $\mathbf{s}$ and $\mathbf{r}$ are given by

$$\mathbf{s}^{\mathrm{T}}=[s_1,s_2,\ldots,s_i,\ldots,s_n],\quad s_i=\frac{z_{i+1}-2z_i+z_{i-1}}{a^2}, \tag{15}$$

$$\mathbf{r}^{\mathrm{T}}=[r_1,r_2,\ldots,r_i,\ldots,r_n],\quad r_i=\frac{s_i}{\sum_{i=1}^{n}\frac{[((z_{i+1}-z_{i-1})/2a)^2+1]^{3/2}}{EA_i}}, \tag{16}$$

a being the length of finite difference discretization.

The eigenvectors obtained by solving the eigenproblems (11) and (12) are orthonormalized with respect to the mass matrix. To alleviate expressions, the v and w indices denoting in-plane and out-of-plane vibration will be dropped when there is no risk of confusion.

3. Program validation

The finite difference formulation described has been programmed and linked to general purpose eigenproblem solvers. To validate the computer program developed, the first three in-plane and out-of-plane frequencies of the main span cable of the Tsing Ma Suspension Bridge are computed. The geometric and mechanical properties of the cable were reported by Xu et al. [7] based on design drawings. The length and sag of the main span cable are 1397.8 and 112.5 m, respectively. Other properties include the cross-sectional area $A=0.759\,\mathrm{m}^2$, modulus of elasticity $E=200\,\mathrm{GPa}$, mass per unit length $m=5832\,\mathrm{kg/m}$, and a horizontal component of the tension force $H_s=122.64\,\mathrm{MN}$. In the absence of relevant data, the moment of inertia is calculated herein based on the gross area of the cable although this assumption is somewhat conservative [1], each of the cables being in fact made of 91 strands of parallel galvanized steel wires [7]. The cable is divided into 100 finite difference elements.

Tables 1 and 2 list the in-plane and out-of-plane frequencies computed using the finite difference program developed and those obtained by Ni et al. [6] based on a finite element modelling. Calculations are carried out using both assumptions of pinned and fixed end supports. Measurements from a series of ambient vibration tests on the same bridge as described in Refs. [6,8] are also presented. Comparison of the results reveals that the frequencies computed using the program developed agree well with those obtained by the finite element formulation or from measurements. This comparison validates the accuracy of the programmed finite difference formulation. In the subsequent sections, this program is used to investigate free vibrations of locally damaged suspended cables.

Table 1
Comparison of in-plane frequencies of the main span cable of the Tsing Ma Suspension Bridge (Hz)

Modes	Fixed ends		Pinned ends		Measurements[b]
	FD[a]	FEM[b]	FD[a]	FEM[b]	
1	0.1048	0.1020	0.1038	0.1008	0.1020
2	0.1505	0.1488	0.1473	0.1471	0.1430
3	0.2100	0.2091	0.2080	0.2081	0.2070

[a]Computed using the finite difference program developed.
[b]Reported in Ref. [6].

Table 2
Comparison of out-of-plane frequencies of the main span cable of the Tsing Ma Suspension Bridge (Hz)

Modes	Fixed ends		Pinned ends		Measurements[b]
	FD[a]	FEM[b]	FD[a]	FEM[b]	
1	0.0524	0.0528	0.0519	0.0522	0.0530
2	0.1048	0.1052	0.1038	0.1040	0.1050
3	0.1573	0.1578	0.1558	0.1557	0.1560

[a]Computed using the finite difference program developed.
[b]Reported in Ref. [6].

4. Cable models

As mentioned before, only recently have research efforts been concentrated on studying the interaction between sag, bending stiffness and cable vibrations [1,4–6]. This interaction has generally been investigated by defining two dimensionless parameters ξ and λ^2 characterizing the bending stiffness and sag-extensibility, respectively

$$\xi = L\sqrt{\frac{H_s}{EI}}, \tag{17}$$

$$\lambda^2 = \frac{EAL}{H_s L_e}\left(\frac{mgL}{H_s}\right)^2, \tag{18}$$

where L_e is a length a little larger than the cable span, defined by

$$L_e = \int_0^L \left(\frac{\mathrm{d}s}{\mathrm{d}x}\right)^3 \approx L(1+8f^2) \tag{19}$$

$$\approx L\left[1+\frac{1}{8}\left(\frac{mgL}{H_s}\right)^2\right] \tag{20}$$

and where f defines the sag-to-span ratio.

The bending stiffness parameter, ξ, measures the relative importance of cable and beam actions: when ξ is very small, beam action predominates, and when ξ is very large, cable action is predominant. Flexural rigidity has generally been ignored in most cable problems characterized by a large ξ parameter [1]. Cables with moderate-to-large diameters as those used for suspension bridges are however characterized by small to moderate ξ parameters and bending stiffness effects should be taken into account in their analysis, especially when accurate modelling is needed as for their structural identification [6].

Table 3
Geometric and mechanical properties of the investigated cables

Cable no.	m (kg/m)	E (Pa)	A (m^2)	I (m^4)	H (N)	λ^2	ξ
1	350	1.60×10^{10}	7.85×10^{-3}	5.00×10^{-6}	2.90×10^{6}	0.60	602.68
2	350	1.60×10^{10}	7.85×10^{-3}	1.50×10^{-5}	2.90×10^{6}	0.60	347.96
3	350	1.60×10^{10}	7.85×10^{-3}	3.00×10^{-4}	2.90×10^{6}	0.60	77.81
4	400	2.00×10^{11}	2.85×10^{-3}	5.00×10^{-7}	3.00×10^{6}	3.24	547.72
5	400	2.00×10^{11}	2.85×10^{-3}	1.50×10^{-6}	3.00×10^{6}	3.24	316.23
6	400	2.00×10^{11}	2.85×10^{-3}	3.00×10^{-5}	3.00×10^{6}	3.24	70.71
7	4	6.45×10^{10}	6.00×10^{-4}	7.00×10^{-9}	1.92×10^{4}	83.75	652.11
8	4	6.45×10^{10}	6.00×10^{-4}	2.10×10^{-8}	1.92×10^{4}	83.75	376.50
9	4	6.45×10^{10}	6.00×10^{-4}	4.20×10^{-7}	1.92×10^{4}	83.75	84.19
10	380	2.00×10^{11}	7.85×10^{-3}	2.00×10^{-7}	1.00×10^{6}	214.47	500.00
11	380	2.00×10^{11}	7.85×10^{-3}	6.00×10^{-7}	1.00×10^{6}	214.47	288.68
12	380	2.00×10^{11}	7.85×10^{-3}	1.20×10^{-5}	1.00×10^{6}	214.47	64.55

The sag-extensibility parameter, λ^2, also known as the Irvine or sag-independent parameter [1], accounts for combined axial and geometric stiffness effects. Geometric stiffness originates mainly from sag and angle-of-inclination of the cable. A detailed discussion of these effects can be found in Ref. [1], but it is worth mentioning that, based on a literature survey, Johnson et al. [9] concluded about some typical values of λ^2: from 0 to 4 for stay cables on cable-stayed bridges, around 90 for overhead transmission lines and in the range of 140–350 for the main cables of suspension bridges.

To cover a wide range of cases within the framework of the present research, cable models with the same span length $L = 100\,\text{m}$ and different combinations of sag-extensibility and bending stiffness parameters are studied to evaluate the effect of damage on their dynamic behaviour. Results are presented for 12 cables with the geometric and mechanical characteristics listed in Table 3. Each cable is subdivided into 100 equi-length elements, generating 101 nodes for each finite difference model.

5. Numerical results

5.1. Study parameters

It is expected that an induced damage to the cable affects its frequencies and mode shapes, but it is not clear how definite are the trends of such influence. In the following sections, this interaction is investigated through examination of the effects of damage location and size on the first in-plane and out-of-plane frequencies and mode shapes of the cable.

Damage is induced in each cable model by locally reducing its cross-sectional area and moment of inertia, to simulate a section loss or a stiffness degradation. It is, however, assumed that the cable mass matrix remains unchanged after damage. The damage location is defined by the dimensionless coordinate ratio x_d/L, where x_d is the distance from cable origin to the damaged section, as illustrated in Fig. 1.

Comparison between the damaged cases and a reference undamaged case is carried out by calculating a frequency percentage change ω_i^* and an eigenparameter $\boldsymbol{\phi}_i^*$ defined by

$$\omega_i^* = \frac{\widetilde{\omega}_i - \omega}{\omega} \times 100, \tag{21}$$

$$\boldsymbol{\phi}_i^* = \frac{\widetilde{\boldsymbol{\phi}}_i}{\widetilde{\omega}_i^2} - \frac{\boldsymbol{\phi}}{\omega^2}, \tag{22}$$

where ω and $\boldsymbol{\phi}$ are the first in-plane (or out-of-plane) frequency and corresponding mode shape, $\widetilde{\omega}_i$ and $\widetilde{\boldsymbol{\phi}}_i$ denote the damaged cable first in-plane (or out-of-plane) frequency and corresponding mode shape when damage is introduced at element i of the cable model. It is worth mentioning that the eigenparameter $\boldsymbol{\phi}^*$ was successfully used to study the vibrations of damaged beam structures as described in Ref. [10].

5.2. Effect of damage location

Using the finite difference scheme programmed by the author, the eigenparameters defined in Section 5.1 are determined for damage located in turn at each of the 100 finite difference elements of each cable model. For purpose of comparison, all cable models are subjected to the same intensity of damage by locally reducing the cross-sectional area by 50% and the corresponding moment of inertia by 75%. Owing to space limitations, results are presented only for damage located at distances $x_d = 0.1L$, $x_d = 0.2L$, $x_d = 0.3L$, $x_d = 0.4L$ and $x_d = 0.5L$ from the cable support. In-plane and out-of-plane vibration sensitivity to damage are discussed separately in the next two subsections.

5.2.1. In-plane vibration

Table 4 contains the percentage change of the first in-plane frequency as a function of damage location. These results are also illustrated in Fig. 2. By comparing the natural frequencies of the damaged and undamaged cables, it can be seen that the first in-plane frequency of cables with small bending stiffness ξ (cables 3, 6, 9 and 12) increases when damage is induced, while for the other cables with medium and high bending stiffness, the first in-plane frequency decreases for the same type of damage. The magnitude of relative change depends on damage location, bending stiffness and sag-extensibility. By examining the curves in Fig. 2, two general trends can be identified:

- For cables with small sag-extensibility (cables 1–6), the curves exhibit a monotonic change in first in-plane frequency when damage location varies from $x_d = 0.1L$ to $x_d = 0.5L$. It is noted, however that the rate of this change increases as sag-extensibility decreases. In other terms, for cables with high bending stiffness (cables 1 and 4 for example), damage occurring either at midspan or near one of the supports, will produce slightly the same decrease in their first in-plane frequency. Conversely, the first in-plane frequency of a cable with a small bending stiffness (cables 3 and 6) damaged at midspan is around 4–6% times higher than its frequency when damaged near the support. It is also interesting to note that for this type of cable, damage effect is maximum when it occurs at midspan, with corresponding relative change varying from about -0.02% for cable 1 to about 6.5% for cable 6 as shown in Table 4. By comparing the percentage frequency change values listed in Table 4, it is clear that for a given bending stiffness, the effect of damage on the first in-plane frequency increases as sag-extensibility decreases. Finally, since all the curves are symmetric about

Table 4
Percentage change in the first in-plane frequency as a function of damage location

Cable no.	$x_d = 0.1L$	$x_d = 0.2L$	$x_d = 0.3L$	$x_d = 0.4L$	$x_d = 0.5L$
1	−0.0240	−0.0248	−0.0259	−0.0269	−0.0273
2	−0.0252	−0.0327	−0.0427	−0.0511	−0.0543
3	0.3685	1.7575	3.7096	5.5281	6.2967
4	−0.1041	−0.1043	−0.1051	−0.1061	−0.1065
5	−0.0983	−0.1014	−0.1101	−0.1188	−0.1224
6	−0.0229	0.8851	2.3920	3.8820	4.5278
7	−0.0011	−0.0028	−0.0028	−0.0011	0.0000
8	−0.0090	−0.0240	−0.0241	−0.0092	0.0000
9	1.9667	6.4453	6.9853	2.2274	0.0000
10	−0.0030	−0.0079	−0.0080	−0.0030	0.0000
11	−0.0253	−0.0676	−0.0680	−0.0261	0.0000
12	1.3062	4.5498	5.4781	2.0081	0.0000

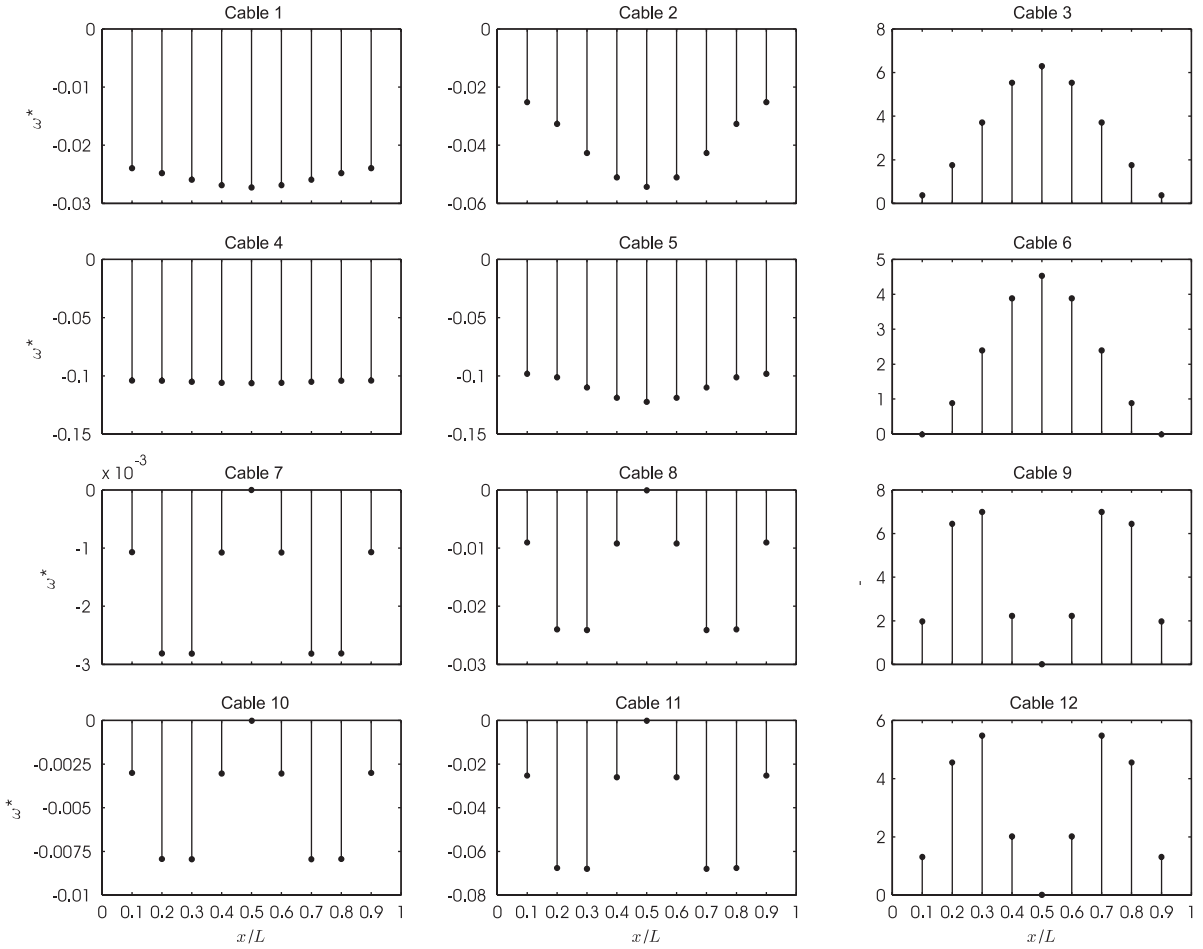

Fig. 2. Percentage change in the first in-plane frequency as a function of damage location.

cable midspan, damage occurring at symmetric locations about this point yield the same effect on first in-plane frequency.

- For cables with medium to high sag-extensibility (cables 7–12), the curves indicate a non-monotonic change in the first in-plane frequency when damage location varies from $x_d = 0.1L$ to $0.5L$. As can be seen, the relative change in frequency is maximum when damage is located around $x_d = 0.25L$, and zero when damage occurs at the middle of the cable span, meaning that a damage located midspan has no effect on the first in-plane frequency. Again, all the curves are symmetric about the middle of the cable span but also almost symmetric about $x_d = 0.25L$, thus whether damage is located at $x_d = 0.2L$, $x_d = 0.3L$, $x_d = 0.7L$ or $x_d = 0.8L$ will have the same effect on first in-plane frequency. Maximum relative change varies from about -0.003% for cable 7 to about 7.0% for cable 9. As for cables 1–6, comparison of the percentage frequency change values listed in Table 4 reveals that for a given bending stiffness, the effect of damage on the first in-plane frequency globally increases as bending stiffness decreases.

Further understanding of these responses can be gained by examining the relationship between in-plane frequencies of symmetric and antisymmetric mode shapes on one hand, and bending stiffness and sag-extensibility parameters on the other. Mehrabi and Tabatabai [5] and Ni et al. [6] developed relation surfaces of first in-plane frequencies as a function of the λ^2 and ξ parameters based on finite element and finite difference formulations. These studies have shown that for the first in-plane and out-of-plane frequencies, these relation surfaces can be approximated without great loss of accuracy by similar curves developed for

cable vibrations with bending stiffness effects excluded [1,11]. The points of intersection of the curves are referred to as frequency *crossover*, defining the transition of dynamic behaviour of a cable from a taut string to an inextensible chain. Thus the first in-plane vibration mode of cables 7–12 is antisymmetric since their sag-extensibility parameter is larger than the first frequency crossover value $\lambda^2 = (2\pi)^2$. Inducing damage at midspan of cables 7–12 is equivalent to introducing a spring-restrained hinge at a location which coincides with an internal node of the first antisymmetric mode shape. Consequently, such damage has no effect on the dynamic behaviour of cables 7–12 as illustrated in Table 4 and Fig. 2.

It is also important to investigate the effect of damage location on the eigenparameters $\boldsymbol{\phi}_i^*$ defined by Eq. (22). Fig. 3 portrays variations of this parameter when damage is induced at distances $x_d = 0.1L$, $x_d = 0.2L$, $x_d = 0.3L$, $x_d = 0.4L$ and $x_d = 0.5L$ from the origin of each of the 12 cables. Again, the curves display different patterns depending on bending stiffness and sag-extensibility parameters. For cables with small sag-extensibility and high bending stiffness (cables 1 and 4), the eigenparameters are only slightly sensitive to damage location which can be hardly detected even by closer examination of the curves. The eigenparameters of cables with small sag-extensibility and medium bending stiffness (cables 2 and 5) are more sensitive to damage, yet the flat shape of the curves in some cases requires careful reading to get a precise indication of damage location as for cable 5 for example. In fact, when detectable, damage location corresponds to peaks on the eigenparameter curves, and the sharper is the peak, the easier and more exactly

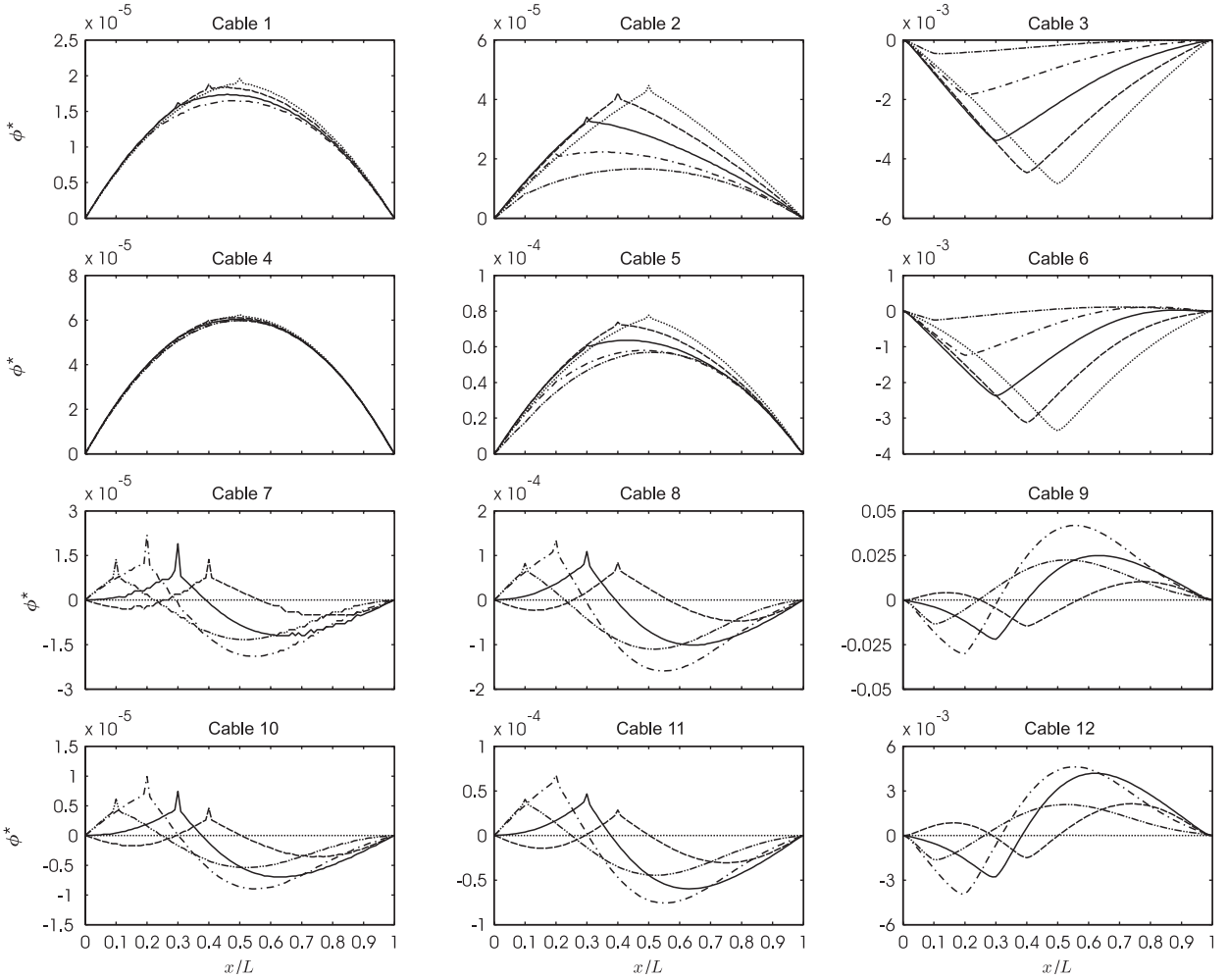

Fig. 3. Effect of damage location on the in-plane mode shape eigenparameter $\boldsymbol{\phi}^*$: –· ·– damage at $x_d = 0.1L$; – · – damage at $x_d = 0.2L$; —— damage at $x_d = 0.3L$; –– damage at $x_d = 0.4L$; · · · · damage at $x_d = 0.5L$.

damage can be located. It is clear from Fig. 3 that sensitivity to damage location increases significantly for cables with small sag-extensibility and bending stiffness (cables 3 and 6) and cables with medium to high sag-extensibility independently of their bending stiffness (cables 7–12). Damage location can indeed be easily

Table 5
Percentage change in the first out-of-plane frequency as a function of damage location

Cable no.	$x_d = 0.1L$	$x_d = 0.2L$	$x_d = 0.3L$	$x_d = 0.4L$	$x_d = 0.5L$
1	−0.0004	−0.0014	−0.0027	−0.0038	−0.0042
2	−0.0034	−0.0124	−0.0235	−0.0326	−0.0360
3	0.4531	1.9276	3.9425	5.7943	6.5714
4	−0.0006	−0.0021	−0.0040	−0.0055	−0.0061
5	−0.0049	−0.0179	−0.0341	−0.0472	−0.0522
6	0.3941	1.7502	3.5876	5.2633	5.9614
7	−0.0003	−0.0011	−0.0020	−0.0028	−0.0031
8	−0.0025	−0.0091	−0.0172	−0.0238	−0.0264
9	0.5421	2.2481	4.6037	6.8055	7.7440
10	−0.0008	−0.0030	−0.0057	−0.0078	−0.0087
11	−0.0069	−0.0255	−0.0487	−0.0674	−0.0746
12	0.3555	1.6775	3.4535	5.0711	5.7437

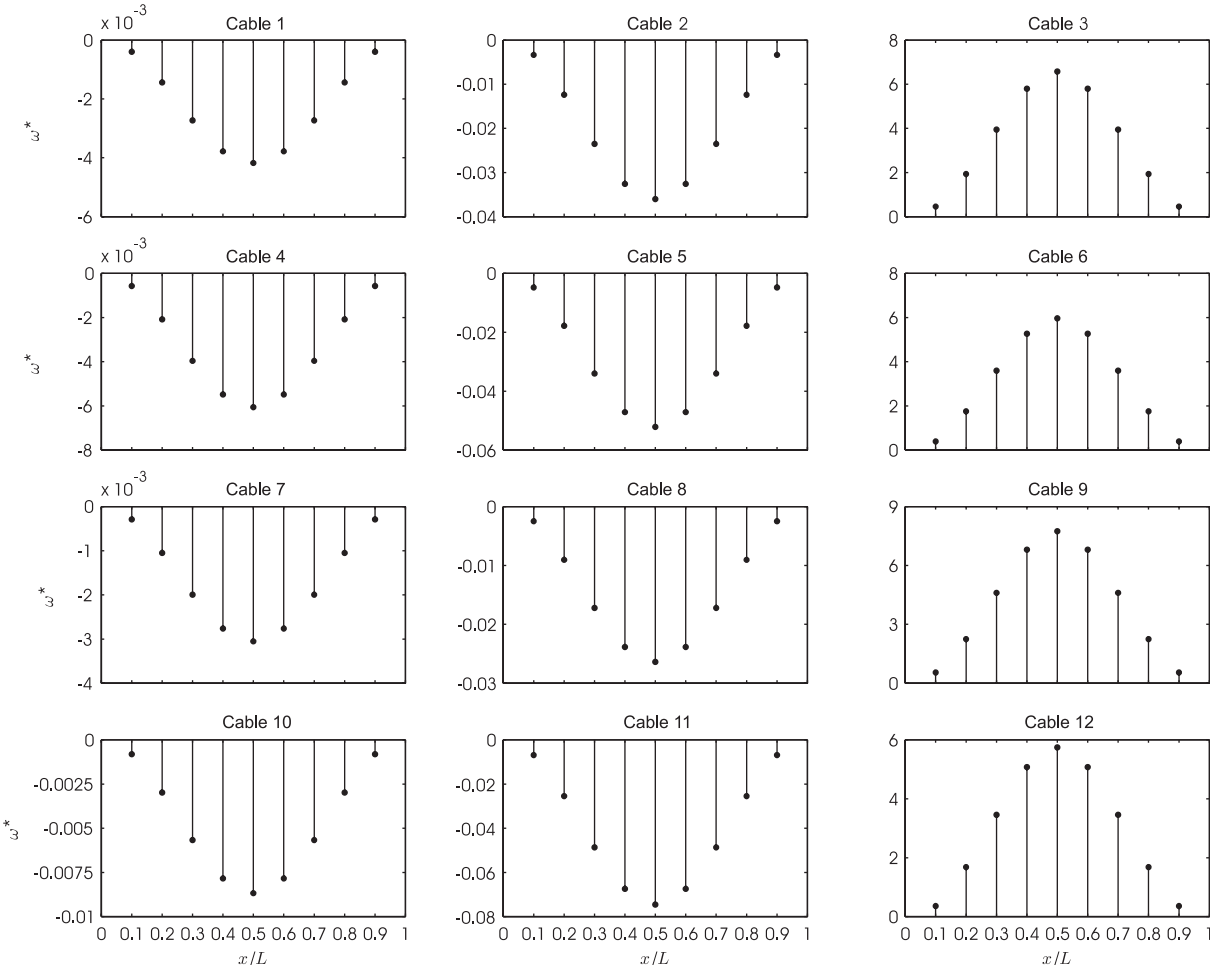

Fig. 4. Percentage change in the first out-of-plane frequency as a function of damage location.

and clearly identified by peaks on the corresponding curves, except when this location is at midspan, leading to $\boldsymbol{\phi}_i^* = 0$ along the cable. This observation confirms that the mode shapes and frequencies corresponding to damage introduced at midspan remain in fact unchanged after damage since midspan coincides with an internal mode shape node as explained before. It is also observed that the $\boldsymbol{\phi}_i^*$ curves of cables 7–12 do not have a constant sign, which is another consequence of the antisymmetric modes.

5.2.2. Out-of-plane vibration

The same systematic procedure described in the previous section is applied to study the effect of damage location on out-of-plane vibration. Table 5 presents percentage change values of the first out-of-plane frequency as a function of damage location. These results are also illustrated in Fig. 4. As for in-plane vibration cases, the induced damage yields an increase in the first out-of-plane frequencies of cables with small bending stiffness and a decrease in the frequencies of cables with medium to high bending stiffness. However, it is noted that the percentage changes follow the same trend for all the cables since there is no frequency crossover phenomenon. The figure shows a monotonic frequency change when damage location varies from $x_d = 0.1L$ to $x_d = 0.5L$, with a maximum being reached when damage is at midspan. It is also noted that the rate of frequency change against damage location is much less sensitive to sag-extensibility than for in-plane

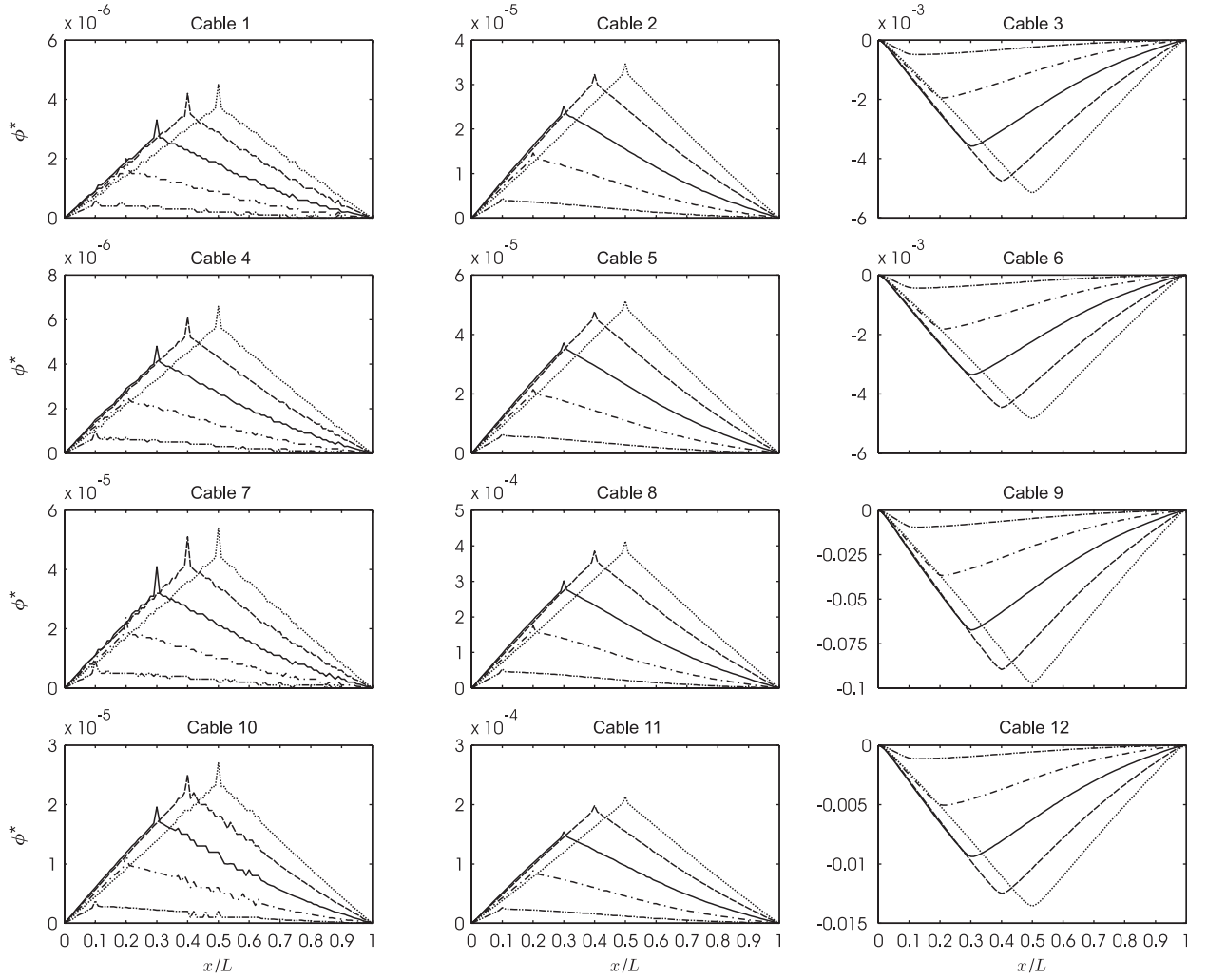

Fig. 5. Effect of damage location on the out-of-plane mode shape eigenparameter $\boldsymbol{\phi}^*$: –··– damage at $x_d = 0.1L$; – · – damage at $x_d = 0.2L$; —— damage at $x_d = 0.3L$; – – damage at $x_d = 0.4L$; · · · damage at $x_d = 0.5L$.

vibration. Thus, for the 12 cables, a damage occurring at mid span produces a frequency change of the order of 3 times that generated if damage has occurred near the support. By comparing the frequency values listed in Table 5, it can again be concluded that for a given bending stiffness, the effect of damage on the first out-of-plane frequency increases as sag extensibility decreases. Fig. 4 also indicates that damage occurring at symmetric locations about cable midspan produces the same effect on the first out-of-plane frequency.

The effect of damage location on the out-of-plane eigenparameters ϕ_i^* is illustrated in Fig. 5 for damage induced at distances $x_d = 0.1L$, $x_d = 0.2L$, $x_d = 0.3L$, $x_d = 0.4L$ and $x_d = 0.5L$ from the left support of each of the 12 cables. Again, the curves display the same patterns independently of the bending stiffness and sag-extensibility. As can be seen, for all the cables, damage location can be clearly identified by pronounced peaks irrespectively of the damage case considered, sag-extensibility or bending stiffness parameters. This is a very important feature of out-of-plane vibration that should be advantageously exploited for condition assessment of suspended cables. Furthermore, it is also observed that the ϕ_i^* curves of all studied cables keep a constant sign along the cable span.

5.3. *Effect of damage size*

The numerical results discussed in Section 5.2 were obtained for a given damage size induced in turn at different locations on the cables, by applying a 50% reduction of the cross-sectional area and 75% reduction

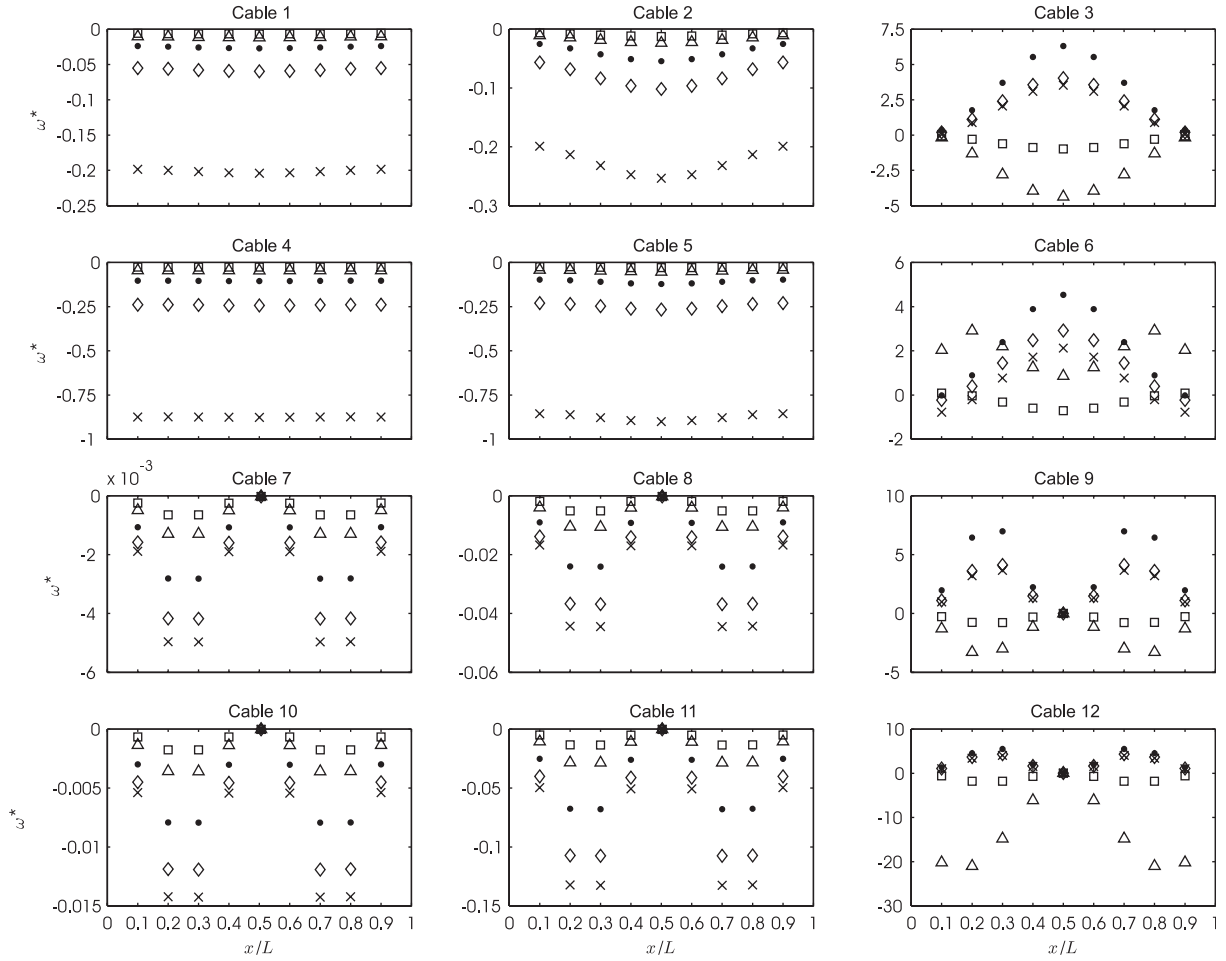

Fig. 6. Effect of damage size on the percentage change in the first in-plane frequency: × damage case 1; ◇ damage case 2; • damage case 3; △ damage case 4; □ damage case 5.

of the moment of inertia. The aim of this section is to study the effect of damage intensity on the modal behaviour of the cables. Damage size is varied by applying a 90%, 70%, 50%, 30% and 10% reduction of the cross-sectional area, and corresponding 81%, 49%, 25%, 9% and 1% reduction of the moment of inertia. These damage cases will be labelled 1–5, respectively. The results obtained are discussed next for in-plane and out-of-plane vibrations separately.

5.3.1. *In-plane vibration*

Fig. 6 illustrates the in-plane frequency percentage change for all the cables when a damage of variable size occurs at locations $x_d = 0.1L$, $x_d = 0.2L$, $x_d = 0.3L$, $x_d = 0.4L$ and $x_d = 0.5L$ from cable support. For cables 1, 2, 4 and 5, characterized by small sag-extensibility and moderate to high bending stiffness parameters, it is seen that all damage cases produce a decrease in the first in-plane frequency. Damage case 1 produces the highest percentage change, followed by damage cases 2, 3, 4 and 5 in decreasing order of importance. It is interesting to note that for the four cables, the ratio of the percentage change produced by damage case 1 to that resulting from damage case 2 is almost constant. Ratios between the percentage changes produced by the other damage cases are also fairly constant. Fig. 6 shows that the same observations are true for cables with moderate to high sag-extensibility and bending stiffness parameters (cables 7, 8, 10 and 11), but taking into

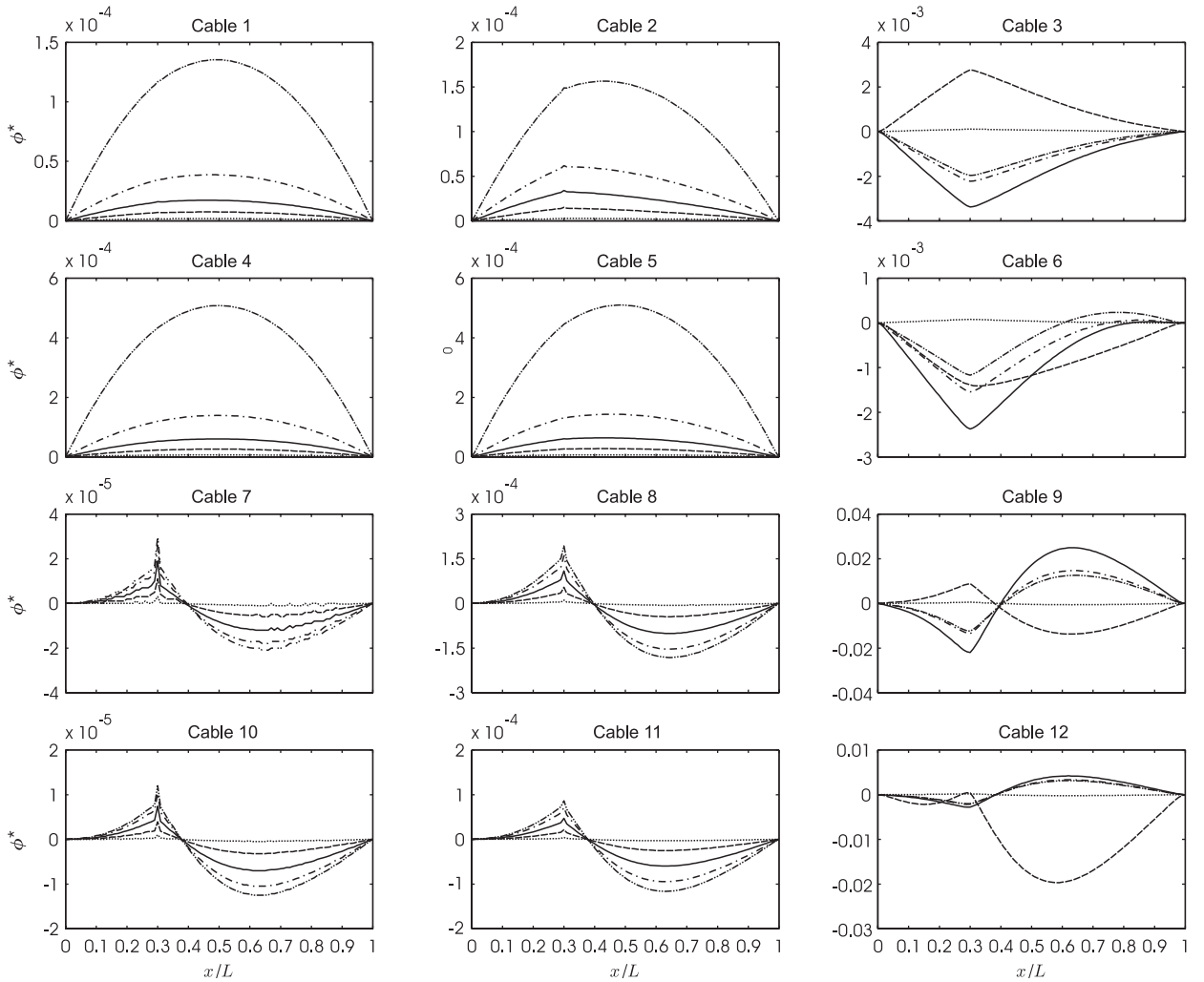

Fig. 7. Effect of damage size on the in-plane mode shape eigenparameter $\boldsymbol{\phi}^*$: —··— damage case 1; — · — damage case 2; —— damage case 3; —— damage case 4; · · · · damage case 5.

account the antisymmetry of the first in-plane mode shape. All damage cases have no effect on the first in-plane frequency when localized at midspan, as discussed before. Cables 3, 6, 9 and 12, characterized by a small bending stiffness parameter, exhibit a completely different trend however. For example, the in-plane frequency of cable 3 decreases under damage cases 4 and 5, and increases under damage cases 1–3. It is also observed that maximum frequency change is now associated to damage case 3 instead of damage case 1 as seen in the previous cases. The response of cable 6 is quite similar to that of cable 3, except under damage case 4 when variations of ω_i^* against damage location are no longer monotonic. For cables 9 and 12, all damage cases at midspan have no effect on the in-plane frequency because of mode shape antisymmetry, but it is observed that in-plane frequencies are amplified under some damage cases as shown for cable 4 under damage case 4. In fact, for small ξ parameters, beam action is predominant and bending effects become locally significant. Consequently, frequencies are highly sensitive to variations of the moment of inertia resulting in rapid changes in curvature similar to those encountered near load points, studied elsewhere using perturbation methods for example [1,12].

The effect of damage size on the $\boldsymbol{\phi}^*$ eigenparameter is illustrated in Fig. 7. The curves represent variations of the $\boldsymbol{\phi}^*$ eigenparameter along cable span for a variable size damage occurring at $x_d = 0.3L$ from the left support of each of the 12 cables. It is clear from the figure that, for cables with small or moderate sag-extensibility and moderate to high bending stiffness, the findings discussed under Section 5.2.1 are valid for all damage sizes studied. It is also noted that the curves are sharp enough to identify damage location. It is also

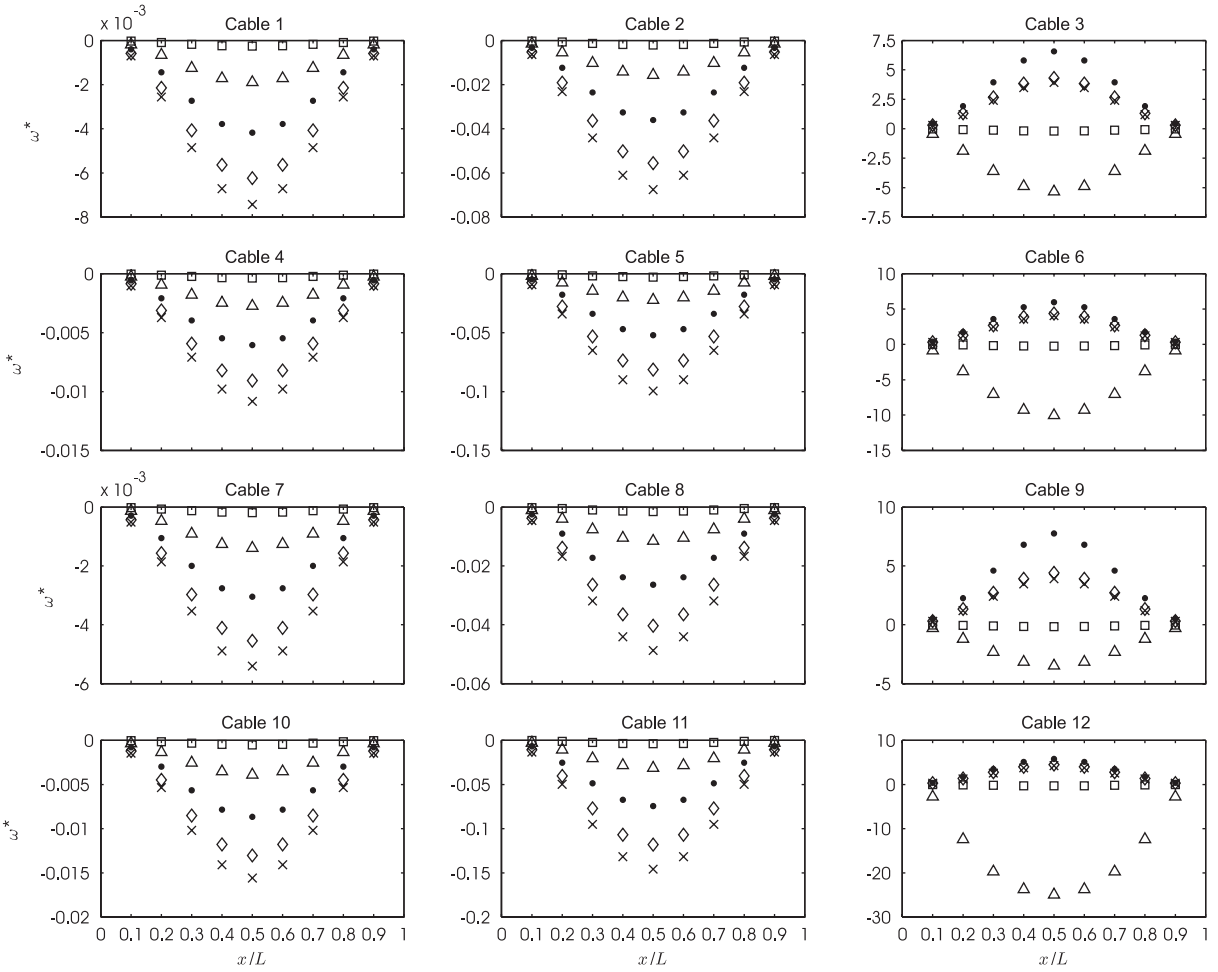

Fig. 8. Effect of damage size on the percentage change in the first out-of-plane frequency: × damage case 1; ◇ damage case 2; • damage case 3; △ damage case 4; □ damage case 5.

noted that all the curves have the same pattern, and that damage case 1 yields the highest $\boldsymbol{\phi}^*$ eigenparameter, followed by damage cases 2, 3, 4 and 5 in this order. As for the frequency parameter ω^*, the eigenparameter curves for cables with a small bending stiffness parameter are highly sensitive to moment of inertia variations and follow complex trends.

5.3.2. *Out-of-plane vibration*

Variations of the out-of-plane frequency change parameter ω^* for all the cables when a damage of variable size occurs at different locations $x_d = 0.1L$, $x_d = 0.2L$, $x_d = 0.3L$, $x_d = 0.4L$ and $x_d = 0.5L$ from cable support are presented in Fig. 8. The figure clearly shows that for cables with small or moderate sag-extensibility and moderate to high-bending stiffness parameters, all damage cases result in a decrease of the first in-plane frequency. Again, damage case 1 produces the highest percentage change, followed by damage cases 2, 3, 4 and 5 in this order. Since the ratios between the percentage changes resulting from the different damage cases are roughly constant, this result can be exploited to estimate damage size for this type of cables. Obviously, this argument can be used for all damage locations because of the symmetry of the first out-of-plane mode shape. For the same reasons discussed above, cables 3, 6, 9 and 12, characterized by a small sag-extensibility, exhibit a different behaviour, but less complex than that for in-plane vibration.

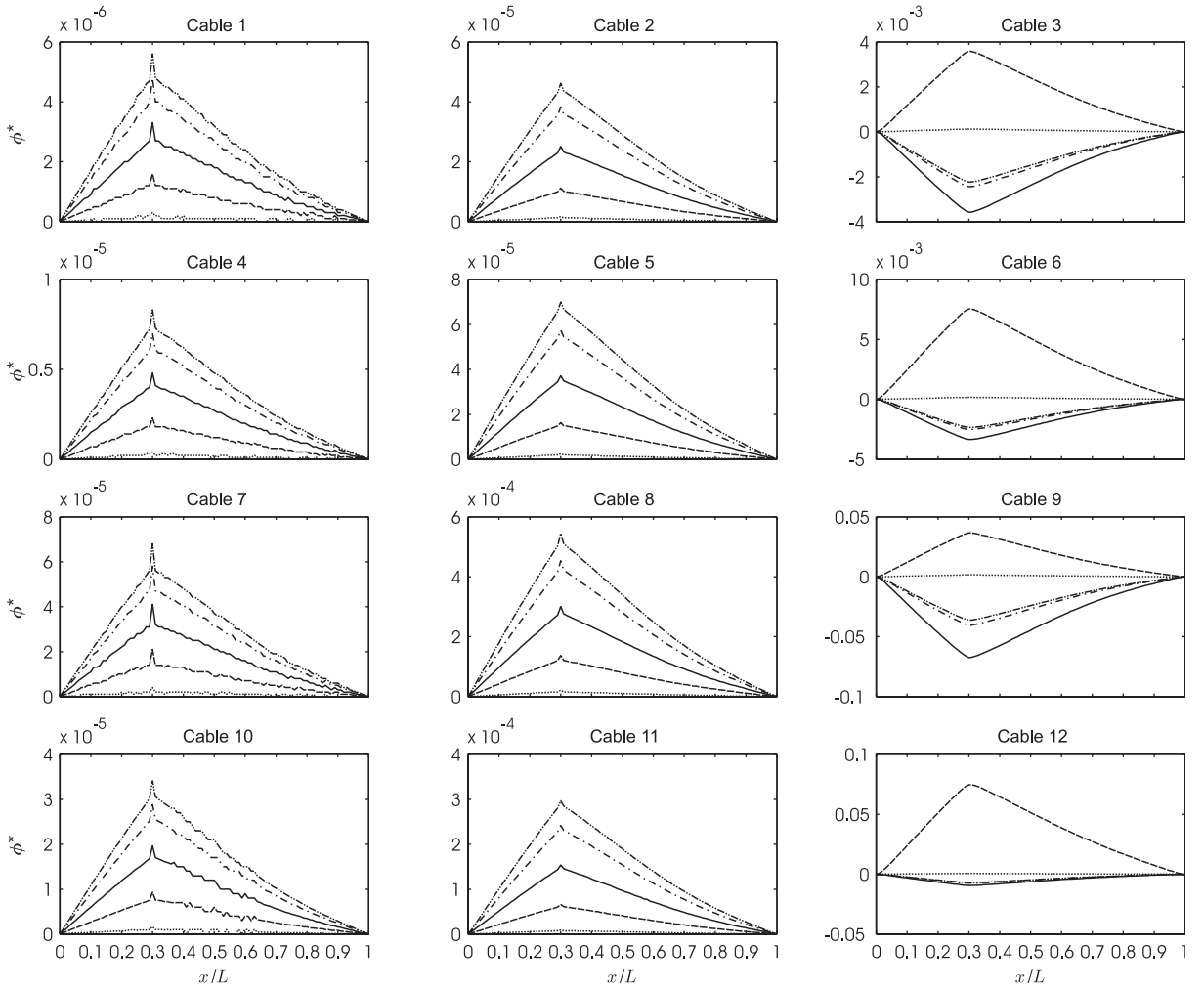

Fig. 9. Effect of damage size on the out-of-plane mode shape eigenparameter $\boldsymbol{\phi}^*$: —··— damage case 1; – · – damage case 2; —— damage case 3; —— damage case 4; · · · · damage case 5.

Fig. 9 portrays the effect of damage size on the out-of-plane ϕ^* eigenparameter. The curves represent variations of the ϕ^* eigenparameter along cable span for a variable size damage occurring at $x_d = 0.3L$ from the left support of each of the 12 cables. Its is apparent from the figure that for cables with small or moderate sag-extensibility and moderate to high bending stiffness, the findings discussed under Section 5.2.1 are valid for all damage sizes studied. It is also observed that damage location is readily apparent on the curves of each of these cables. The curves have the same pattern, and damage case 1 yields the highest ϕ^* eigenparameter, followed by damage cases 2, 3, 4 and 5 in decreasing order of importance. Again, as discussed for the frequency percentage changes, cables with a small bending stiffness are highly sensitive to moment of inertia variations and their trends are difficult to track.

6. Concluding remarks

The present paper was primarily intended to numerically investigate the interaction between damage location, damage size and the modes of vibration of simple suspended cables. For this purpose, a finite difference formulation originally developed elsewhere for studying in-plane vibration of cables is extended herein to investigate out-of-plane vibration as well. The finite difference scheme, which includes sag and bending stiffness effects, is programmed and adapted to study locally damaged suspended cables. An extensive parametric study is conducted for twelve types of cables with different combinations of sag-extensibility and bending stiffness parameters. Percentage change in the first in-plane and out-of-plane frequency and the corresponding eigenparameter characterizing mode shapes are defined to determine the dynamic behaviour of the cables under various damage cases. The orders of magnitude of these parameters are shown to be closely related to the cable parameters. It is clearly shown that despite the complexity of the relationship between damage and the dynamic properties of the cables, some definite trends could be identified, especially for out-of-plane vibration. It is important to mention that the present study was carried out under the simplified assumption of decoupled in-plane and out-of-plane motions and that only single damage scenarios were considered. Extending the results of this study to cover more complex cases would require further investigation.

References

[1] H.M. Irvine, *Cable Structures*, The MIT Press, Cambridge, 1981.
[2] G. McClure, Dynamic analysis of cable structures: a review, Report No EPM/RT-86-12, Department of Civil Engineering, École Polytechnique de Montréal, Montreal, 1986 (in French).
[3] G. Zheng, Vibration-based Condition Assessment of Cables in Cable Supported Bridges, Ph.D. Dessertation, Department of Civil and Structural Engineering, The Hong Kong Polytechnic University, Hong Kong, 2002.
[4] H. Zui, T. Shinke, Y. Namita, Practical formulas for estimation of cable tension by vibration method, *Journal of Structural Engineering* 122 (1996) 651–656.
[5] A.B. Mehrabi, H. Tabatabai, Unified finite difference formulation for free vibration of cables, *Journal of Structural Engineering* 124 (1998) 1313–1322.
[6] Y.Q. Ni, J.M. Ko, G. Zheng, Dynamic analysis of large-diameter sagged cables taking into account flexural rigidity, *Journal of Sound and Vibration* 257 (2) (2002) 301–319.
[7] Y.L. Xu, J.M. Ko, Z. Yu, Modal analysis of tower-cable system of Tsing Ma long suspension bridge, *Engineering Structures* 19 (10) (1997) 857–867.
[8] J.M. Ko, Y.Q. Ni, J.Y. Wang, Tsing Ma suspension bridge: ambient vibration survey campaigns, *Proceedings of the International Conference on Advanced Problems in Vibration Theory and Applications*, Xi'an, China, 2000, pp. 285–291.
[9] E.A. Johnson, R.E. Christenson, B.F. Spencer Jr., Semiactive damping of cables with sag, *Computer-Aided Civil and Infrastructure Engineering* 18 (2) (2003) 132–146.
[10] M.M.F. Yuen, A numerical study of the eigenparameters of a damaged cantilever, *Journal of Sound and Vibration* 103 (3) (1985) 301–310.
[11] A.S. Veletsos, G.R. Darbre, Free vibrations of parabolic cables, *Journal of Structural Engineering* 109 (2) (1983) 503–519.
[12] J.D. Cole, *Perturbation Methods in Applied Mathematics*, Blaisdell, Waltham, MA, 1968.